[논 문] 한국재료학회지
Korean Journal of Materials Research
Vol. 13, No. 2 (2003)

Physical/Chemical Characterization of Ordinary Portland Cement/Ground Granulated Blast Furnace Slag Pastes Containing Low Carbon Steel as Reinforcements

Jin-Ha Hwang†
Department of Materials Science and Engineering
College of Engineering
Hongik University 72-1 Sangsu-Dong, Mapo-Gu, Seoul 121-791 KOREA

(2003년 1월 6일 받음, 2003년 2월 10일 최종수정본 받음)

Abstract The interface between low carbon steel and blended cement pastes containing slag was investigated using impedance spectroscopy. In addition, the pastes were characterized by several analytical methods (XRD, EDX, electrode potential, pH and ICP). The electrical behavior of the interface in the blended slag systems is correlated to its corresponding pore solution chemistry and the products present in the interface. Passivation occurred at the paste/steel interfaces, in cement pastes up to containing from 0 to 75% slag content. 100% slag paste induced corrosion of the low carbon steel, which could be explained by the influence of sulfur on the system.

Key words impedance spectroscopy, slag, cement, passivation, sulfur

1. Introduction

The use of ground granulated blast furnace slag (GGBFS) as a replacement material for ordinary Portland cement(OPC) lowers hydration heat, reduces permeability, and enhances resistance to sulfate and chlorine attack, but also significantly changes the chemistry of the paste.[1-4] Corrosion is an electrochemical phenomenon involving anodic and cathodic reactions between the pore solution and the steel. Corrosion-induced volume expansion in reinforced concrete affects the durability of cement-based materials in structural applications. Since GGBFS is so widely used in the field, knowledge of the effect of slag has on corrosion is extremely significant. Slag should be compatible with low carbon steel, if it is to be used in combination with reinforcing materials.

Impedance spectroscopy (IS) has been gaining widespread use as a nondestructive electrical analysis technique in cement-related research for the characterization of the bulk cement paste and the interface between reinforcing steel and cement paste.[5-8] Impedance spectroscopy has also been employed to understand the effect of chloride and sulfate ions on corrosion.[5,9] The study of the cement/steel interface during early hydration has not been extensively researched using IS, in spite of the effect of these initial reactions on the later service stage. The corrosion behavior of OPC-GGBFS mixtures has been suggested based on data from SEM and potentiodynamic polarization, but has not been analyzed directly.[10] The effectiveness of GGBFS cement in reinforced concrete is not clearly understood, but GGBFS cements are still widely used in real applications.[10,11] Cement-based materials without slag produce a highly alkaline oxidizing state of the pore solution (pH = 12-13). Therefore, ordinary Portland cement generates stable phase (preferred high valence state, Fe^{3+}, Fe_2O_3) at the steel/paste interface as a passive thin layer that retards further degradation.

In this work, the chemistry of the pore solution, the electrical behavior and the phase composition of the paste/steel interface were investigated in GGBFS-cement pastes as a function of hydration time and composition. The implications on corrosion are discussed.

2. Experimental Procedure

GGBFS (provided by Koch Minerals Company, Chicago, Illinois) was blended with ASTM Type 1 ordinary Portland cement (OPC) in weight ratios of 0, 25, 50, and 75 and mixed at a water/solid (=*w/s*, solid = slag + OPC) ratio of 0.5. The 100% slag was mixed with water at a *w/s* ratio of 0.37 in order to minimize shrinkage. The chemical information of the GGBFS and the OPC is shown in Table 1. The pastes were cast into polycarbonate molds with dimensions of 2.54 cm×2.54 cm×10 cm or cylindrical containers. Electrodes were inserted directly into the preset pastes. The specimens were kept in a chamber at 100% relative

†E-Mail : jhwang@wow.hongik.ac.kr

Table 1. Chemical analysis of ordinary Portland cement (OPC) and ground granulated blast-furnace slag (GGBFS) based on ICP and XRF.

Oxide	Portland Cement (wt%)	GGBFS (wt%)
SiO_2	10.54	36.35
Al_2O_3	6.02	9.90
CaO	59.93	37.26
MgO	2.73	12.36
Fe_2O_3	2.78	0.28
TiO_2	....	0.79
Na_2O	1.12 (equivalent)	0.30
K_2O	....	0.40
MnO	....	0.68
Sulfur Analyses (%)		
Sulfide	....	1.19
Sulfur-Trioxide	4.77	0.13
Blaine Fineness (cm^2/g)	....	5623

humidity. For pore solution extraction, the above pastes were cast into the cylindrical containers and sealed until the pore solution was extracted. Pore fluid was extracted according to Barneyback and Diamond,[12] and the pH and electrode potential were measured using digital pH meter and a redox combination electrode (Pt-Ag/AgCl), respectively.

C1018 carbon steel rods with diameters of 1/8 and 3/16" (Nak-Man Co., Skokie, Illionis) and plates (McMaster Carr, Elm Hurst, Illionis) were used as electrodes. 3-inch long rods and plates were polished using abrasive papers up to 600 grit. The polished electrodes were cleaned with acetone. Electrodes were cast perpendicular to the field direction.

Extracted pore solutions were also used to determine if corrosion was occurring. The solutions were kept in small bottles. The rod shaped C-1018 electrodes were installed through the top of the bottle so that they were partially submerged in the pore solution, then the top was sealed using transparent silicone rubber sealant. This setup prevented continuous evaporation and carbonation of the pore solution.

Impedance spectra were acquired using a Solatron frequency response analyzer (SI 1260, Schlumberger, Billerica, MA) with "Z60" software.[13] Data were collected at the oscillating amplitude of 25 mV, ranging from 10^6 Hz to 10 mHz or 1 mHz in logarithmic intervals. The IS spectra were corrected to remove inductive and capacitive effects due to the leads and the measurement apparatus.[14] The corrected impedance spectra were analyzed using "*Equivalent Circuit*" *software*.[15] Ionic concentrations of sulfur, sodium, and potassium in the pore solutions were measured using inductively coupled plasma photospectrometry (ICP) (Plasma 40, Perkin-Elmer).

Chemical analysis of the corrosion product produced in the pore solution extracted from the 100% slag paste, was performed using an energy-dispersive X-ray spectrometer, installed in a field emission scanning electron microscope (FESEM S-4500, Hitachi, Japan). X-ray diffraction (XRD) patterns were collected on the surface of the cement paste side of the interface, using an X-ray diffractometer (Rigaku Denki Co., Ltd., Japan). The scanning step was 0.1° with a counting time of 10 sec, in order to obtain reasonable counting statistics from the specimens.

3. Results and Discussion

3.1. Motivation for corrosion study in slag-blended cements.

OPC paste produces a highly alkaline pore solution with an oxidizing potential. Such features accommodate the presence of a passive Fe (III) oxide layer, which retards further oxidation kinetically. The resistive behavior of the

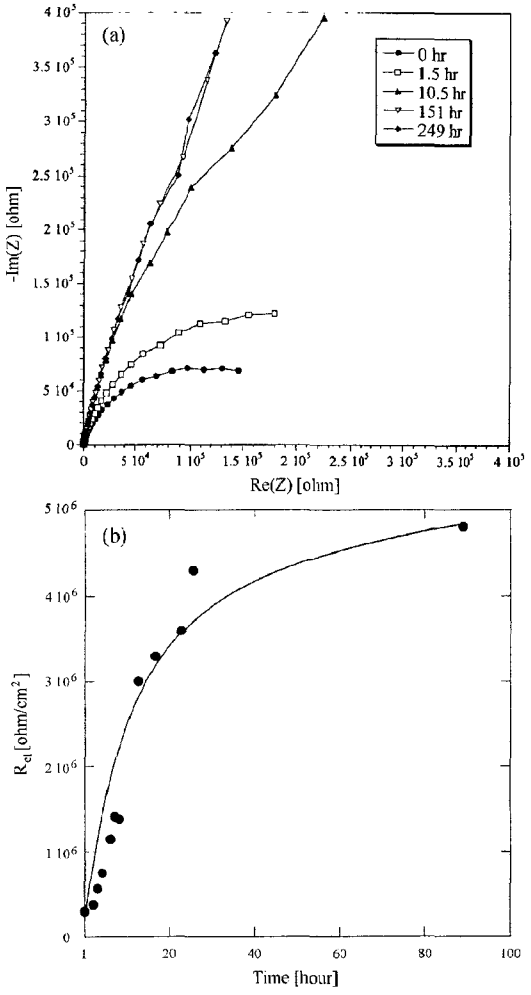

Fig. 1. (a) Impedance spectra and (b) electrode resistance of low 1018 carbon steel in a 3-day OPC extracted pore solution as a function of time. (normalized by electrode area).

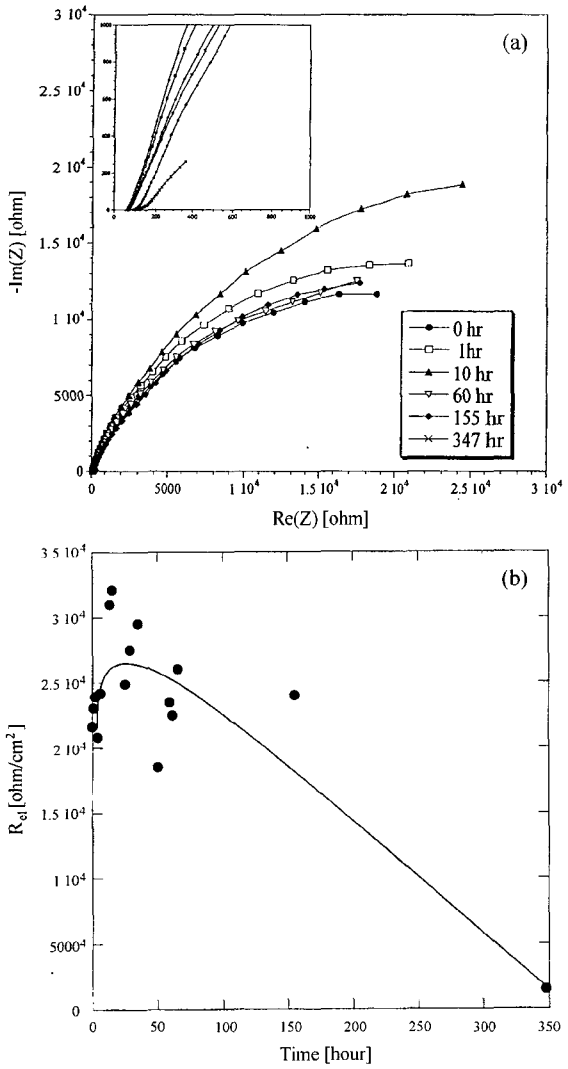

Fig. 2. (a) Impedance spectra and (b) electrode resistance of low 1018 carbon steel in a 7-day GGBFS extracted pore solution as a function of time. (normalized by electrode area).

oxide film in pore solution extracted from 3-day hydrated OPC as a function of time is observed in Fig 1. The resistance increases with immersion time, to 1 day due to the growth of the oxide layer. Unlike OPC, pure GGBFS produces a pore solution with a lower pH (~11.5) and a reducing potential (200~400 mV). In 100% slag-based pore solution, the electrical response exhibited a dissimilar trend as shown in Fig. 2, where the oxide resistance decreased with time. GGBFS pore solution induced severe corrosion, producing a brown-colored corrosion product that was followed by discoloration and the formation of blue-colored gels in the pore solution.

Energy-dispersive X-ray analysis of the metal surface showed a significant amount of sulfer (much higher than the initial amount in the metal as an impurity) and the presence of Mg and Ca in addition to Fe. Since the stability limit of the iron oxide film lies somewhere between these two extremes (100% OPC and 100% GGBFS), the corresponding physicochemical characteristics should be understood for the wide-spread application of these materials in the field. Of those elements that are closely associated with the pore solution chemistry in slag-blended cements, the high level of S (shown in ICP results) appears to activate corrosion.

This dissimilar behavior necessitated the investigation of mixtures of GGBFS and OPC. Initially, C-1018 rods were partially submerged in pore solutions extracted from 7-day hydrated specimens. Unlike that of Fig. 2, the electrical behavior of the oxide layer formed in the blended pastes is similar to that of pure OPC, except for 100%GGBFS. As time increased, the electrode resistance increased, indicating that the oxide layer grew to a certain point. Macphee and CaO[11] reported that in the 85%GGBFS-OPC pore solutions, the electrode resistance decreased and increased at later times. Such upturn was proposed to be associated with the interfacial oxide layer. Actually, the intermediate arc is dependent on the charge transfer at the solution/electrode interface. The experimental condition for the case was not clear.

3.2. Electrical Properties of GGBFS-blended cements

Typical impedance spectra of various blended pastes are shown in Fig. 3. Normally, three arcs can be seen in Nyquist plots for cement paste, as represented by the equivalent circuit model in Fig. 4. In Fig. 3, the frequency increases along the curve from right to left. The high frequency arc is associated with the bulk cement paste, the intermediate arc is governed by charge transfer and double layer capacitance, and the low-frequency arc is associated with the oxide layer formed on the electrode.[6] The high frequency response is dominated by the interconnected pore structure, which controls the diffusivity of ions through the matrix, such as chlorine or sulfur.[6,7] Also, the refined pore structure of blended cement paste limits the diffusion of dissolved oxygen in aerated conditions. In this work, the electrode resistance refers to the fitted resistance of the low frequency arc. The passive film produces a high capacitive value owing to its very thin dimension (5-10 nm).[16]

As shown in Figs. 3 and 5, the total resistance increased with hydration time. Unlike pure OPC and blended-cement pastes, two bulk arcs are developed at the later hydration times in 100% GGBFS pastes. The second arc appears to be related to the formation of the layer structure interconnected pore solution paths, resulting in dielectric amplification. The first of the frequency bulk arcs can be due to

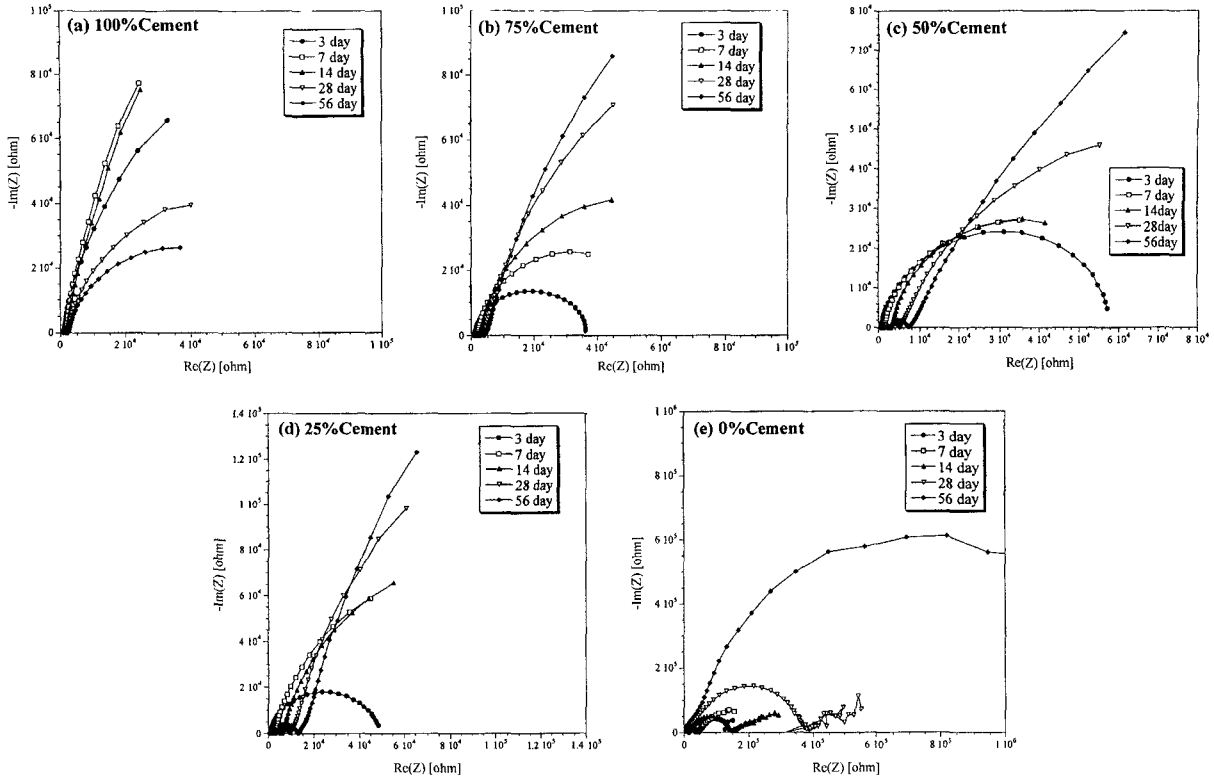

Fig. 3. Impedance spectra at (a) 100% cement, (b) 75% cement-25% slag, (c) 50% cement-50% slag, (d) 25% cement-75% slag, and (e) 100% slag.

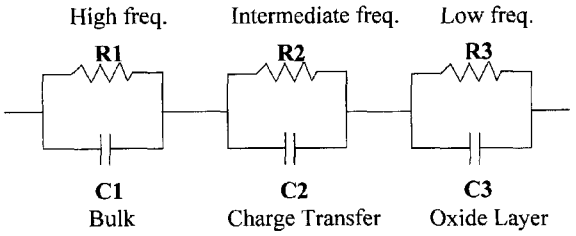

Fig. 4. Equivalent circuit in cement-based materials.

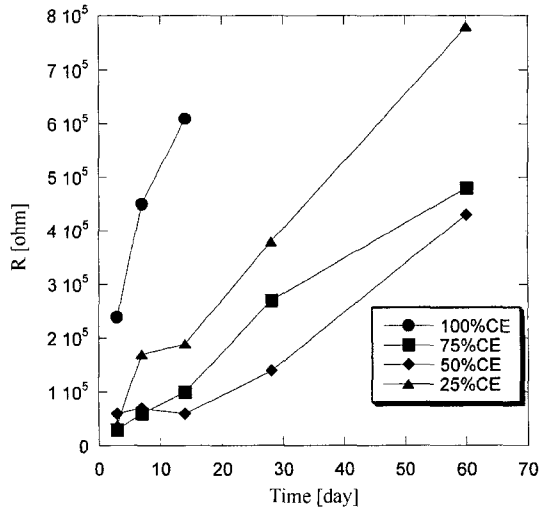

Fig. 5. Electrode resistance vs. hydration time at various ratios of cement to slag.

the restricted resistance of the pore solution at the smaller pores in conjunction with the decreased conductivity of GGBFS pore solution. At early hydration, the GGBFS-based systems displayed a different electrode arc, compared with that of OPC, indicating that the electrode resistance is based on a different mechanism, due to the change in pore solution chemistry or the different composition. The formation of Fe(II) oxide instead of Fe(III) oxide was proposed in slag-based systems,[10] and Naish[17] reported the presence of a magnetite layer in the anaerobic conditions in a cement paste matrix containing slag. However, as the hydration time increased, the electrode resistance of the blended cements continued to increase, from the pore solution work. Although the 100% GGBFS paste exhibited a slanted line, it did not show the 45 slope characteristic of a diffusion-limited process at the electrodes. The surface of the carbon steel that was embedded in the GGBFS paste had a brown-colored corrosion product, which appeared to impede the charge transfer at the interfacial regions, as shown by the scattering of data points in the low frequency arc in Nyquist plot (see Fig. 3(e)).

The electrode resistance of the blended cements increased with hydration time. The possibility of forming Fe_3O_4 in the blended cement and GGBFS pastes can be excluded. The conductivity of Fe_3O_4 in the blended pastes is much higher than that of Fe_2O_3, and the absolute

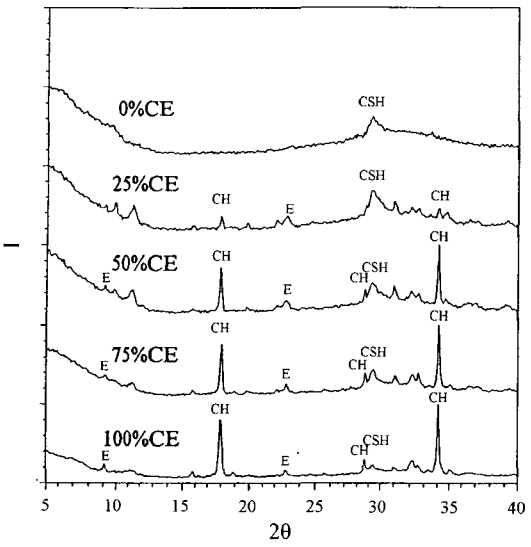

Fig. 6. XRD patterns of specimens of bulk OPC/GGBFS pastes. i) CH: calcium hydroxide, ii) CSH: calcium silicate hydrate, and iii) E: ettringite.

electrode resistance would be much lower in comparison to that of OPC. However, the electrode resistances of the blended cements are within one order of magnitude of OPC, indicating that the oxidation layer based on Fe^{3+}, Fe_2O_3, is formed like that of OPC.

The XRD patterns of the paste side, shown in Fig. 6 displays the presence of various phases as a function of GGBFS content. Except for that of 100% GGBFS, all blended GGBFS-OPC systems exhibited ettringite and higher amount of calcium hydroxide (CH). The relative intensity of calcium silicate hydrate (CSH) tends to increase with GGBFS content. Especially, the presence of ettringite appears to corroborate the buffering capability of OPC against the deteriorating character of GGBFS, resulting in the protection of low carbon steel. The XRD pattern (as not shown here) on the surface next to the electrode seems to have been altered due to carbonation and/or an increased concentration of iron at the steel electrode interface. These issues should be taken into consideration in determining the state of the iron oxide layer with respect to corrosion resistance in the following research efforts.

3.3. Pore solution chemistry of GGBFS-blended cements.

The addition of GGBFS to ordinary Portland cement changes the pore solution chemistry significantly. In Fig. 7(a), the pH is given for GGBFS-blended cements as a function of hydration time. As can be seen, the pH decreases with slag content. This is mainly associated with the deceases in alkali content (K^+, Na^+) (see Fig. 8) and the oxidation of sulfur species.[10] Another significant change in

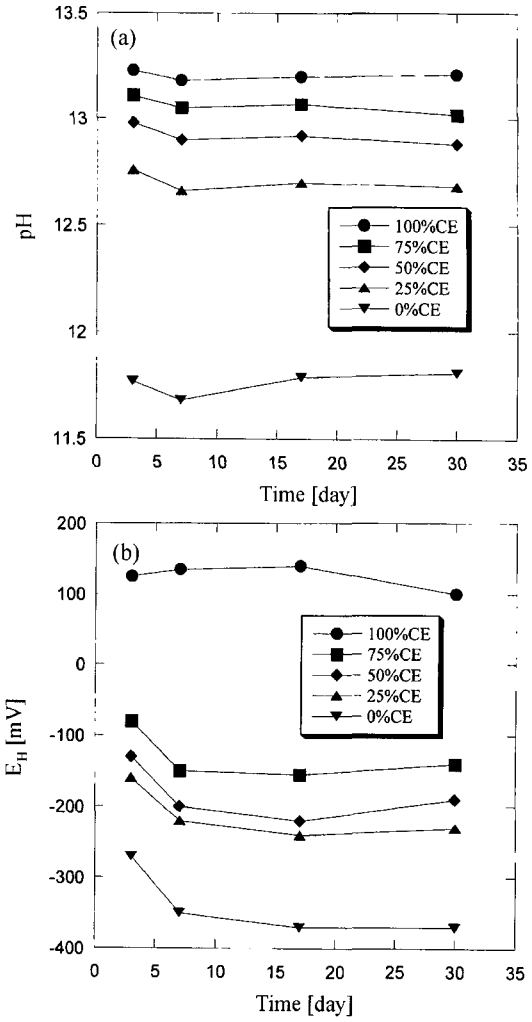

Fig. 7. (a) pH vs. hydration time and (b) E_H vs. hydration time.

the pore solution chemistry is observed in Fig. 7(b). The use of 25% slag to cement induces a reduced state due to the reducing species present in GGBFS. The electrode potential decreases with increasing GGBFS content. The chemical analysis of GGBFS (see Table 1) shows the presence of the reducing species, manganese and sulfur. Although the exact content of reducing species involved cannot be quantified, the addition of slag decreases the electrode potential and also changes the polarity.

Fig. 8 shows the ionic concentration of potassium, sodium, and sulfur vs. time for pore solution extracted from samples of various blends of OPC and GGBFS. The concentration of S in the blended cements appears to be suppressed with respect to that of OPC, while pore solution extracted from GGBFS paste exhibits higher concentrations of S. The decrease in alkali ions with GGBFS contents is noticeable.

As shown in Fig. 7, OPC paste exhibits the oxidizing state, and this is due to the oxidizing state of sulfur, (SO_4^{2-}). The reducing characteristics of slag-based systems are believed to be related mainly to the soluble sulfide ions

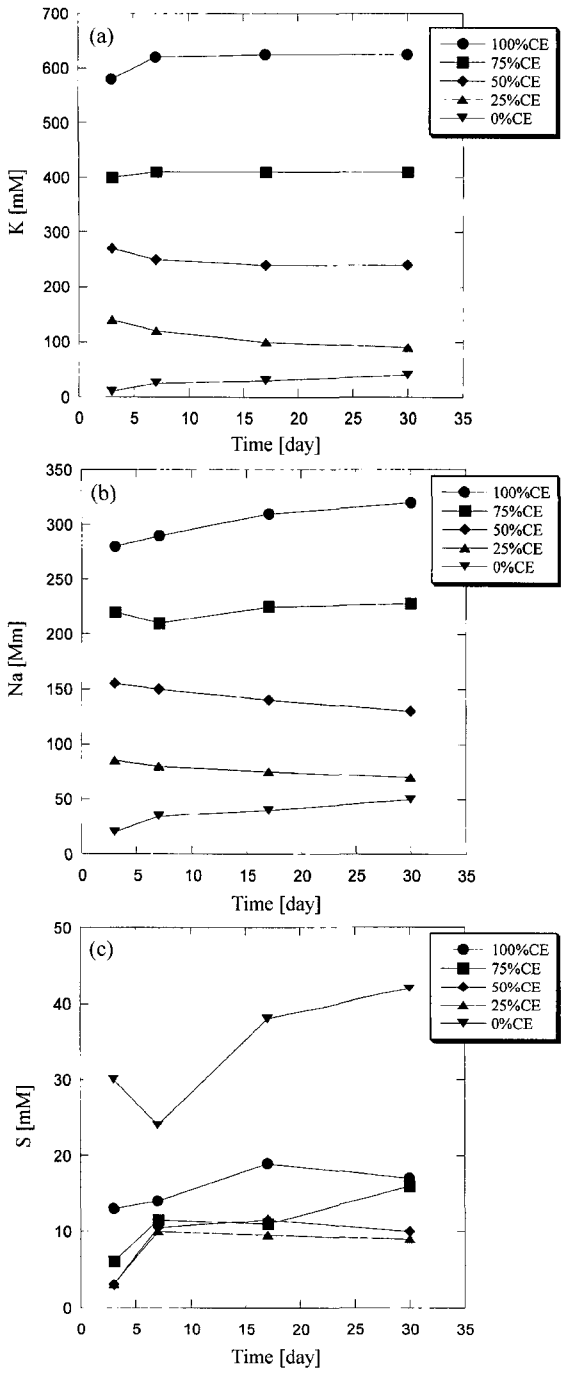

Fig. 8. Concentrations of various ionic species present in pore solution analyzed by ICP. (a) K, (b) Na, and (c) S.

like S^{2-}, HS^-, and S_n^{2-}.[18] The correlation between electrode potential and sulfide contents (S^{2-}) has been reported from ion chromatography analysis of the pore solutions.[18] The amount of S^{2-} was shown to increase with slag content, especially beginning with 80-85% slag replacement. The mixtures of up to 75% slag-blended cements of the current system show that the S^{2-} amount is not enough to induce early corrosion as seen in the GGBFS paste.

Higher oxidizing electrode potential of OPC prefers the presence of higher valence state of Fe^{3+}, Fe_2O_3, as indicated by the iron Pourbaix diagram.[19] In the pore solution extracted from a 7-day OPC paste, significant corroding behavior was not seen in both submerged and unsubmerged parts. Furthermore, the high electrode resistance and its time-dependence supports the above hypothesis, i.e., the presence of the above insulating layer.

The 100% slag pore solutions exhibited dissimilar corrosion behavior above and below the solution. Above the solution, the iron was corroded, while below the solution, the surface was not corroded due to the lack of the oxygen contents caused by the limited reduced state of the pore solution. Possibly, the different behavior can be correlated with the presence of sulfur species. Sulfur species can make the electrode potential of pore solution negative, making the reduced state preferred. Sulfur-based ions such as S^{2-} and SO_3^{2-} have been shown to accelerate the corrosion in reinforced concretes.[20] Apparently, in this very reduced state, hydrogen is evolved and the sulfur species evaporates from the solution as hydrogen sulfide gas, causing the upper portion of the outside of the pore solution to corrode. The experimental conditions simulate the locally-sealed structure in cement pastes where solid and liquid phases coexist within empty pores. This situation is a model where the reinforcement is immersed in the cementitious materials. The evolution of hydrogen sulfide gas may be an important parameter when analyzing the corrosion mechanisms in pastes with high slag content.

Macphee and Cao[10] proposed the possibility of a Fe^{2+} state in the iron oxide layer. Therefore, in 100% GGBFs, the current behavior enables us to propose the presence of Fe_3O_4 or its coexistence with Fe_2O_3. Furthermore, after a certain time (after 150 hour), the system corrodes seriously. Electrode potential and pH are crucial in determining the passivation of the electrodes. As can been in Fig. 7, for up to 75% slag-replaced cement, the pH is maintained above 12.5. However, E_H stays above 100 mV (the oxidized state) in the case of 100% OPC. As the slag is added to cement, pH and electrode potential decreases, changing the polarity of the electrode potential, down to-240 mV. The field is located within the stability region of the Fe_2O_3, but is much closer to the Fe_3O_4 region.[19] The Nyquist plots of Fig. 3 show similar trends and values at 28 days, indicating the same mechanism is operating in this range. However, In case of pure slag, the pH and electrode potential decreased much more. Hence, the pore solution chemistry is much different in comparison to OPC paste. The higher content of sulfur is a major corrosive agent, as evidenced by EDX analysis on corrosion products. In the ICP analysis, the sulfur in GGBFS-blended cements is depressed, compared with that of OPC. Therefore, the effect of sulfur on blended-

cement will be reduced, even with the reduced valence state. Such depression of sulfur is favorable for passivation of reinforcing elements.

4. Conclusion

Impedance spectroscopy and analytical techniques were employed to investigate the corrosion of low carbon steel in GGBFS-blended cements. The stable passivation region was established in both pastes and pore solutions at replacement up to 75% GGBFS. Pure slag pore solution induced severe corrosion products, i.e., a brown colored species made up of Fe, S, Mg, and Ca. The detrimental corrosion appears to be induced by the high concentration of reduced sulfur ions. However, the addition of OPC suppressed the detrimental corroding effect of GGBFS, possibly through the buffering capacity of OPC pore solution. A refined pore structure in slag-blended cements should be beneficial in reinforced cement structures.

Acknowledgment

The author is grateful to R. A. Olson for experimental advise and help, and to Dr. S. J. Ford, Dr. H. M. Jennings, and Dr. T. O. Mason for their useful advise to interpretation of the current data.

References

1. N. Kouloumbi, G. Batis and C. Malami, Cement & Concrete Composites, **16**, 253 (1994).
2. D. Manmohan and P. K. Mehta, Cem. Conc. & Aggregates, **3**(1), 63 (1981).
3. Q. L. Feng, E. E. Lachowski and F. P. Glasser, in Pore Structure and Permeability of Cementitious Materials, Mat. Res. Soc. Symp. Vol.137, Materials Research Society, Pittsburgh, PA, p.419 (1987).
4. M. D. M. Roy and Y. Fang, in Pore Structure and permeability of Cementitious Materials, Mat. Res. Soc. Symp. Vol. 137, Materials Research Society, Pittsburgh, PA, p.403 (1987).
5. P. Gu, Y. Fu and J. J. Beaudoin, Cem. Con. Res, **24**(2), 231 (1994).
6. S. J. Ford and T. O. Mason, in STP 1276 Techniques to Assess the Corrosion Activity of Steel Reinforced Concrete Structures. Philadelphia PA. American Society for Testing and Materials, (1996).
7. B. J. Christensen, R. T. Coverdale, R. A. Olson, S. J. Ford, E. J. Garboczi, H. M. Jennings and T. O. Mason, J. Am. Ceram. Soc., **77**(11), 2789 (1994).
8. H. C. Kim, S. Y. Kim and S. S. Yoon, J. Mat. Sci., **30**, 3768 (1995).
9. T. -P. Cheng, J. -T. Lee and W, -T. Tsai, Cem. Con. Res., **20**, 243 (1990).
10. D. E. Macphee and H. T. Cao, Mag. Con. Res, **45**(162), 63 (1993).
11. R. B. Polder and R. F. M. Bakker, Mag. Con. Res., **46**(167), 151 (1994).
12. R. S. Barneyback, Jr. and S. Diamond, Cem. Concr. Res., **11**, 279 (1981).
13. Scribner Associats, Inc., "Z60" Software for the Schlumberger 1260, Charlottesville, VA 22901 (1996).
14. D. D. Edwards, J. -H Hwang, S. J. Ford and T. O. Mason, Solid State Ionics **99**, 85 (1997).
15. B. A. Boukamp, "Equivalent Circuit (EQIVCRT,PAS)" University of Twente, Dept. of Chemical Technology, P. O. Box 217, 7500 AE Enschede, the Netherlands, (1988).
16. J. E. O. Mayne, J. W. Menter and M. J. Pryor, J. Chem. Soc., **46**(3), 3229 (1950).
17. C. C. Naish, Nirex report NSS/R273 (1990).
18. M. J. Angus and F. P. Glasser, in Scientific Basis for Nuclear Waste Management IX, Mat. Res. Soc. Symp. Vol. 50, Materials Research Society, Pittsburgh, PA, p.547 (1985).
19. M. Pourbaix, Atlas of electrochemical Equilibria in Aqueous Solutions, NACE, Houston, p.263, 312, (1974).
20. N. L. Thomas, J. Mat. Sci., **22**, 3328 (1987).